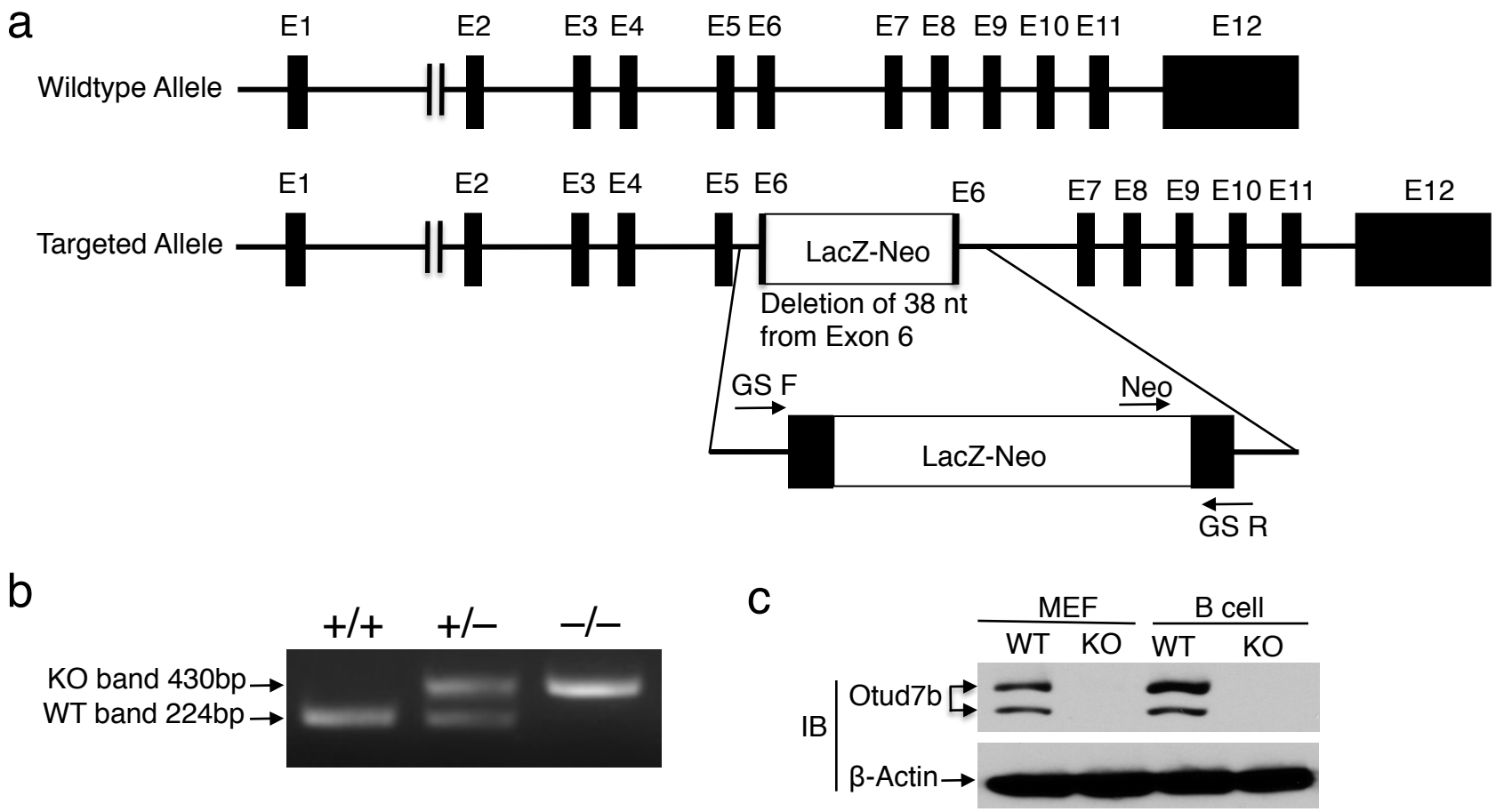

Supplementary Figure 1. *Otud7b* gene targeting. a, *Otud7b* gene locus and targeting strategy. A 38 nucleotide fragment of exon 6 was replaced with a lacZ/neomycin cassette. Genotyping PCR primers for amplifying wildtype (WT) allele (GS F + GS R) and *Otud7b*-KO allele (Neo + GS R) are indicated. **b,** Genomic PCR analysis of WT (+/+), *Otud7b* heterozygous (+/–) and homozygous (–/–) KO mice. **c,** Immunoblotting analysis of whole-cell lysates from WT and KO MEFs or B cells using antibodies for Otud7b or β-Actin. Otud7b were detected as two bands.

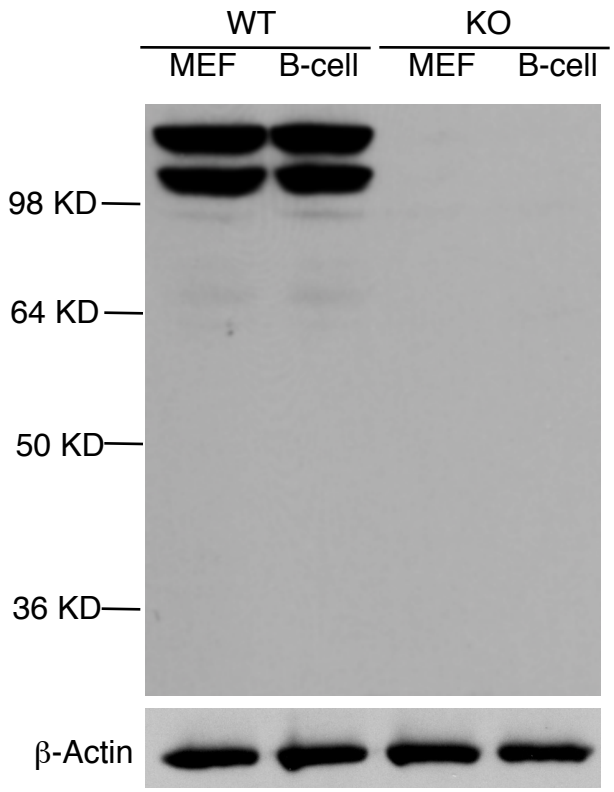

Supplementary Figure 2. *Otud7b* knockout does not generate truncated Otud7b products. IB analyses of Otud7b, showing the entire gel image. The anti-Otud7b antibody was raised against a human Otud7b recombinant protein containing the N-terminal 355 amino acids. This antibody cross reacts with mouse and Rat Otud7b.

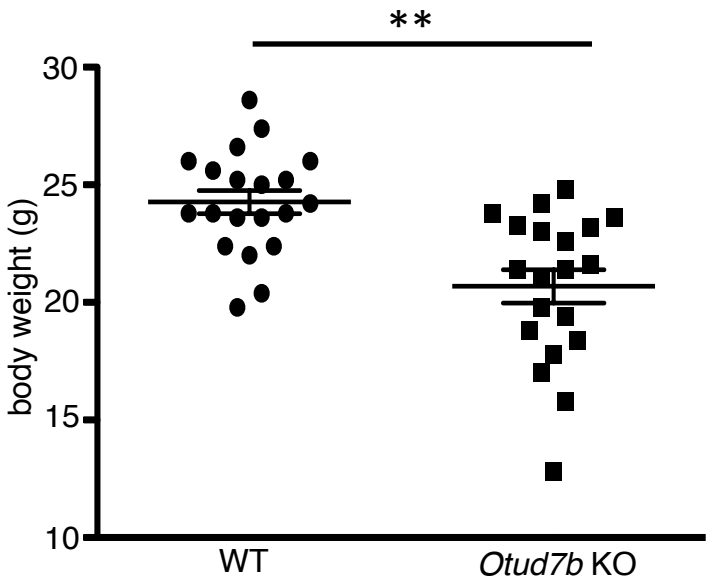

Supplementary Figure 3. *Otud7b* KO mice have reduced body weight. Body weight of WT and *Otud7b* KO mice was measured between the age of 6-8 weeks. Data are presented as mean±SD of multiple mice (each dot represents one mouse). **p<0.01

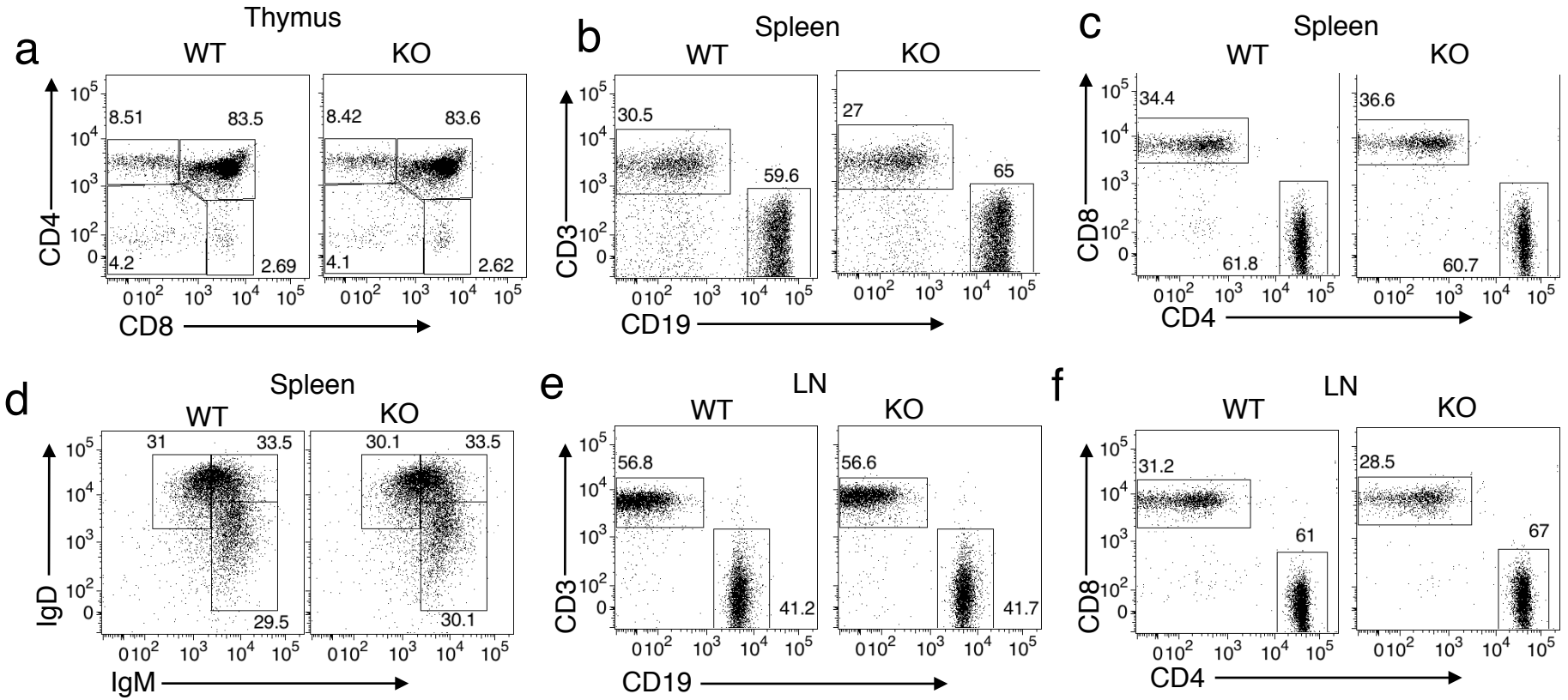

Supplementary Figure 4. ***Otud7b*** **KO mice have normal T and B cell development. a**, Flow cytometry analysis of WT and *Otud7b*-KO (KO) thymocytes based on CD4 and CD8 staining. **b-f,** Flow cytometry analyses of WT and KO splenocytes or lymph node (LN) cells determine the frequency of $CD3^+$ T and $CD19^+$ B cells (**b, e**), CD4 and CD8 T cells (**c, f,** gated on $CD3^+$ cells) and mature ($IgD^{hi}IgM^{low}$) and immature ($IgD^{low}IgM^{hi}$) B cells (**d**, gated on $CD19^+$ cells). Data are representative of three independent experiments, each with three or more mice per genotype group.

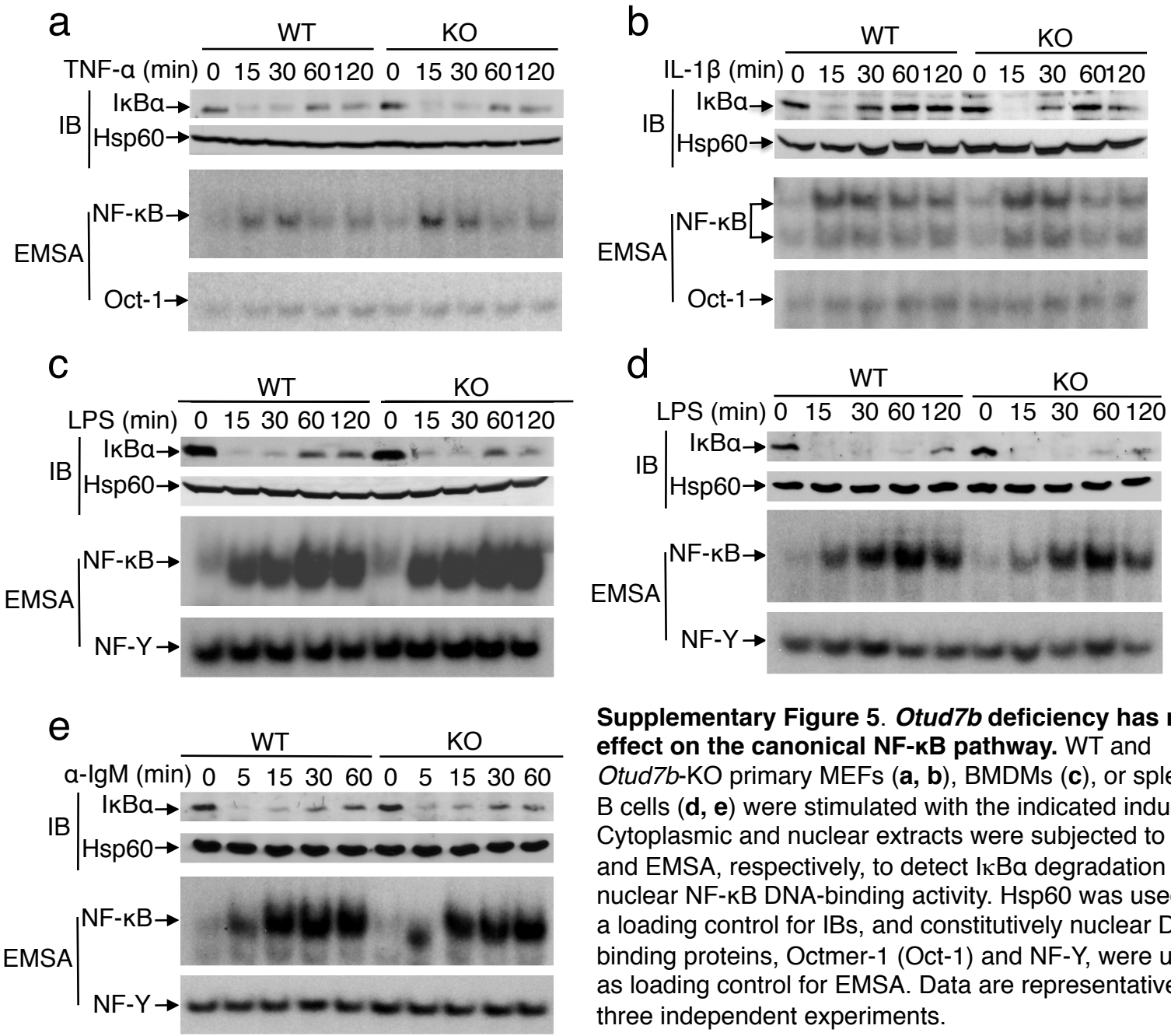

Supplementary Figure 5. ***Otud7b*** **deficiency has no effect on the canonical NF-κB pathway.** WT and *Otud7b*-KO primary MEFs (**a, b**), BMDMs (**c**), or splenic B cells (**d, e**) were stimulated with the indicated inducers. Cytoplasmic and nuclear extracts were subjected to IB and EMSA, respectively, to detect IκBα degradation and nuclear NF-κB DNA-binding activity. Hsp60 was used as a loading control for IBs, and constitutively nuclear DNA-binding proteins, Octmer-1 (Oct-1) and NF-Y, were used as loading control for EMSA. Data are representative of three independent experiments.

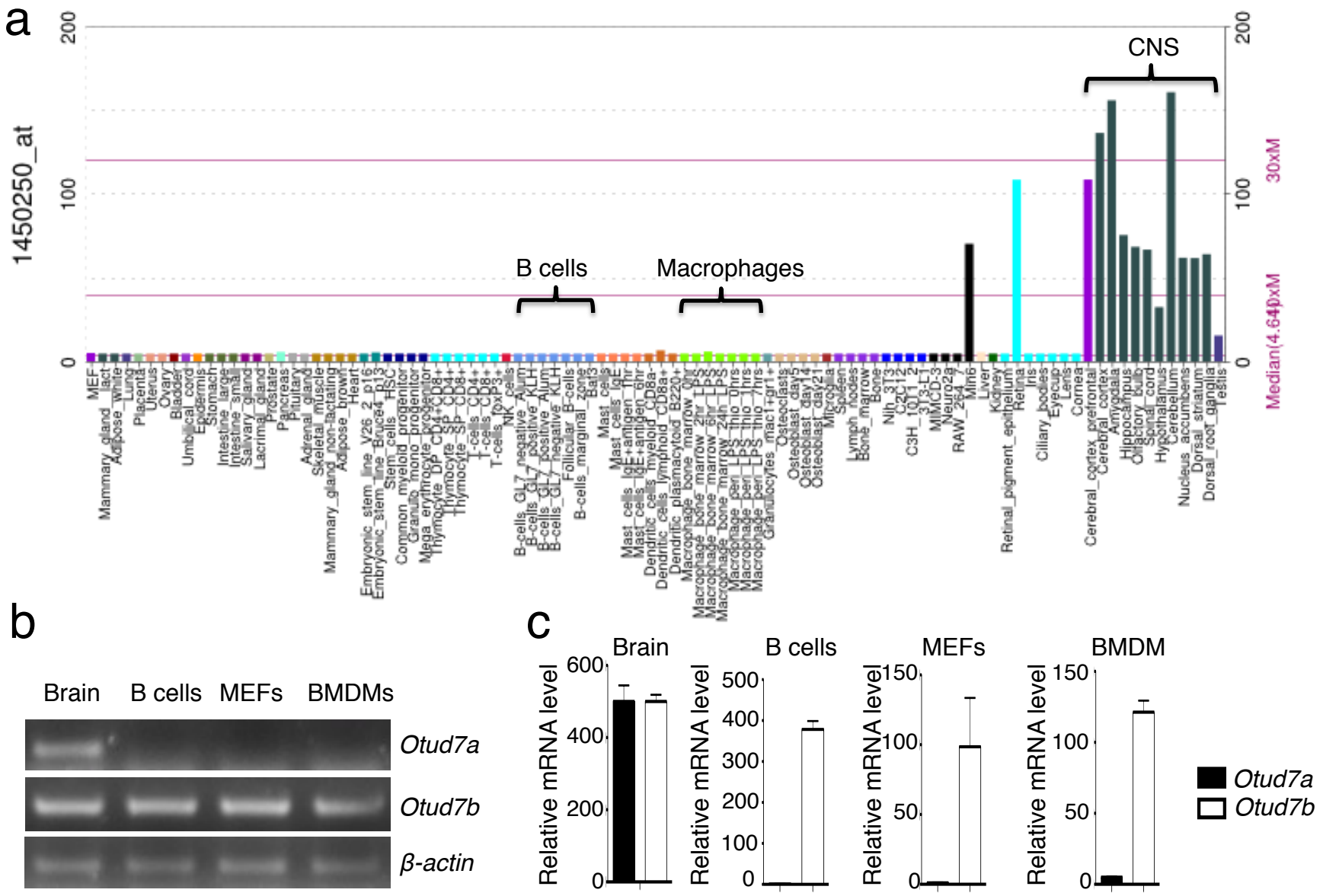

Supplementary Figure 6. **CNS-specific expression of *Otud7a*. a**, *Otud7a* gene expression data from BioGPS. **b, c**, RT-PCR (**b**) and real-time RT-PCR (**c**) analyses of *Otud7a*, *Otud7b*, and *β-actin* mRNA expression in the brain tissue, B cells, mouse embryonic fibroblasts (MEFs), and bone-marrow derived macrophages (BMDMs). Data are representative of two independent experiments.

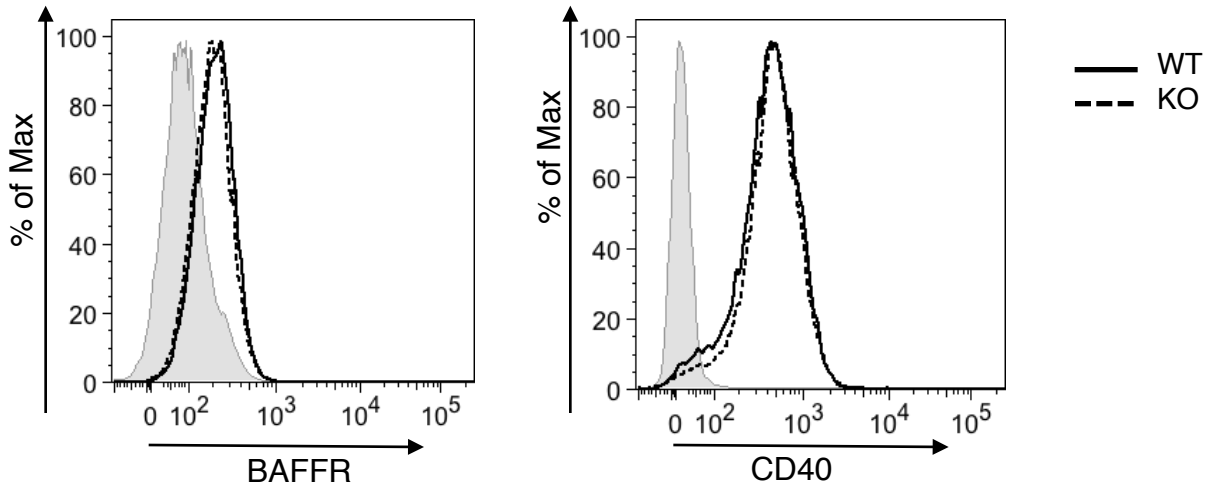

Supplementary Figure 7. WT and *Otud7b* KO B cells have comparable BAFFR and CD40 expression levels. Flow cytometry analysis of the expression level of BAFFR and CD40 on Wildtype (WT) and *Otud7b*-KO (KO) splenic B cells. The gray curve indicates isotype control. Data are representative of three independent experiments, each with three or more mice per genotype group.

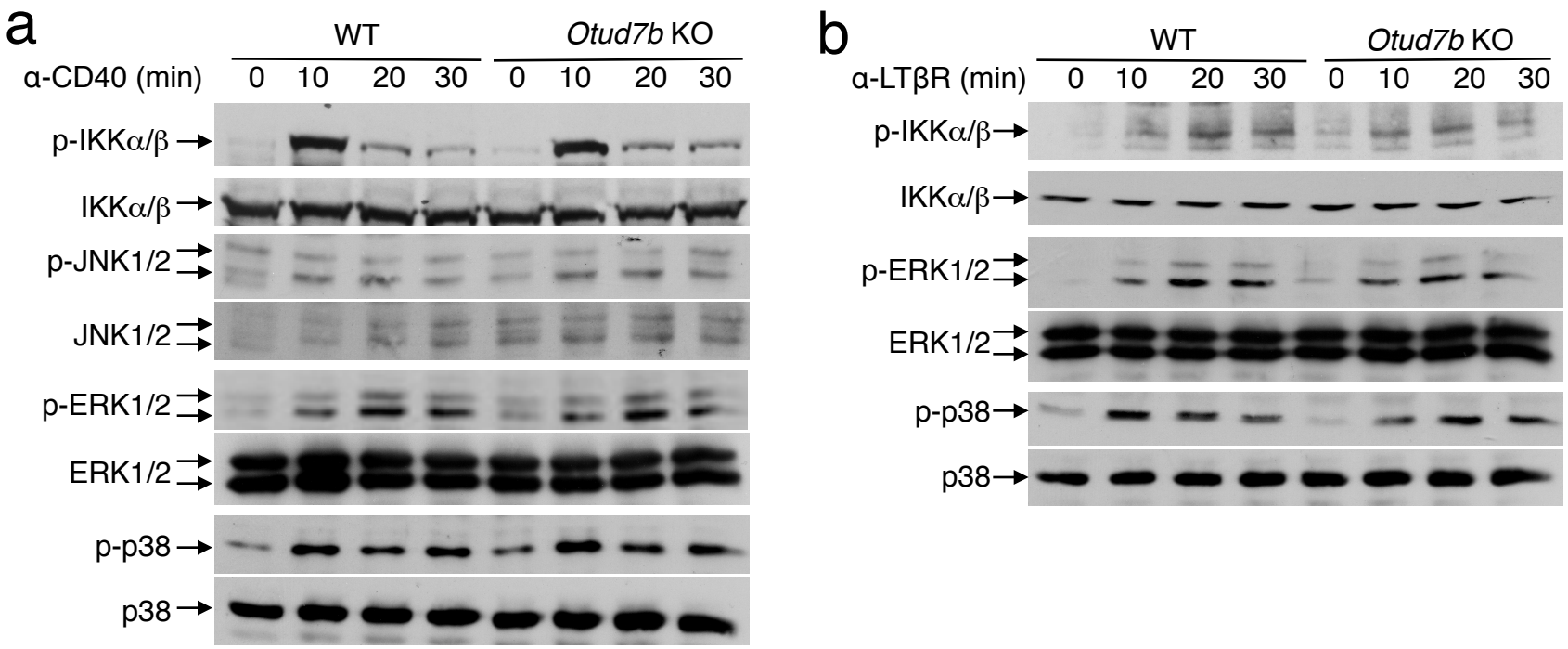

Supplementary Figure 8. Otud7b is dispensable for activation of IKK and MAP kinases by CD40 and LTβR. IB analysis of the indicated phosphorylated (p-) or total proteins in whole-cell lysates of WT or *Otud7b*-KO B cells (**a**) or MEFs (**b**). Data are representative of two independent experiments.

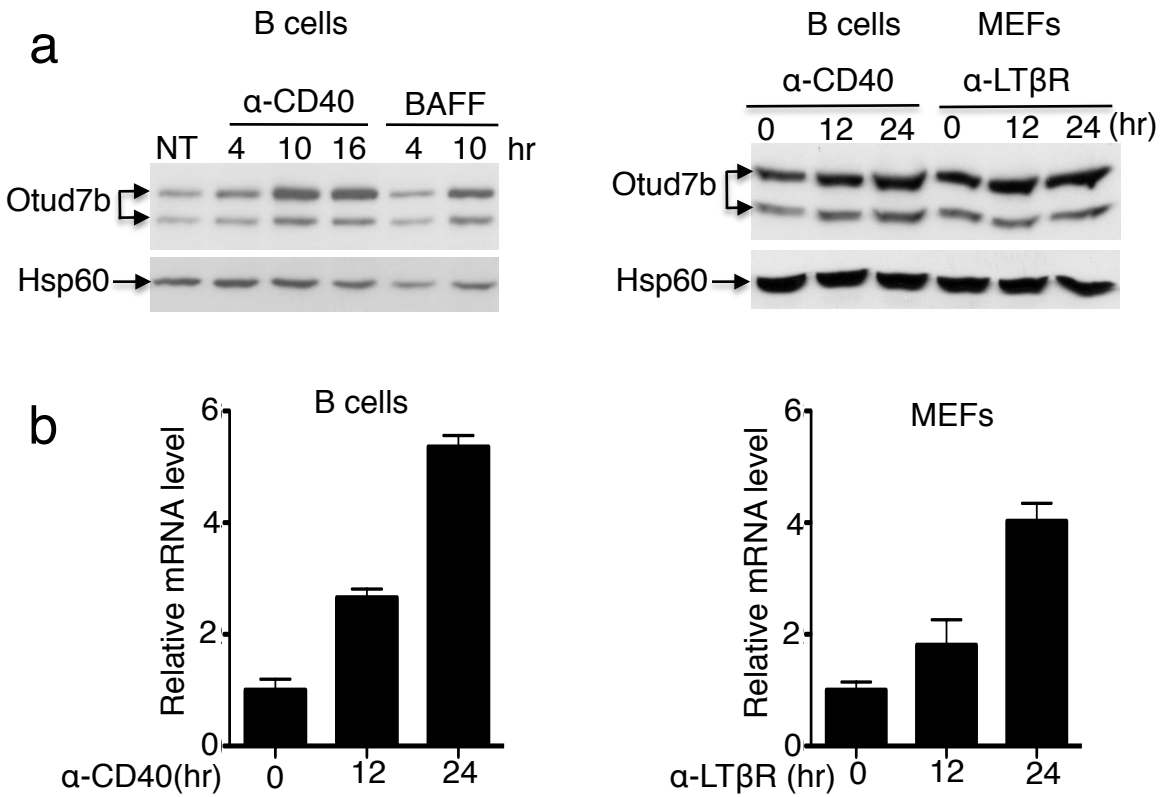

Supplementary Figure 9. Otud7b is induced by noncanonical NF-κB stimuli. a, IB analysis of Otud7b and the loading control Hsp60 in whole-cell lysates of primary B cells and MEFs, stimulated as indicated. **b,** QPCR analysis of *Otud7b* mRNA expression in anti-CD40-stimulated B cells and anti-LTβR-stimulated MEFs. Data are representative of three independent experiments.

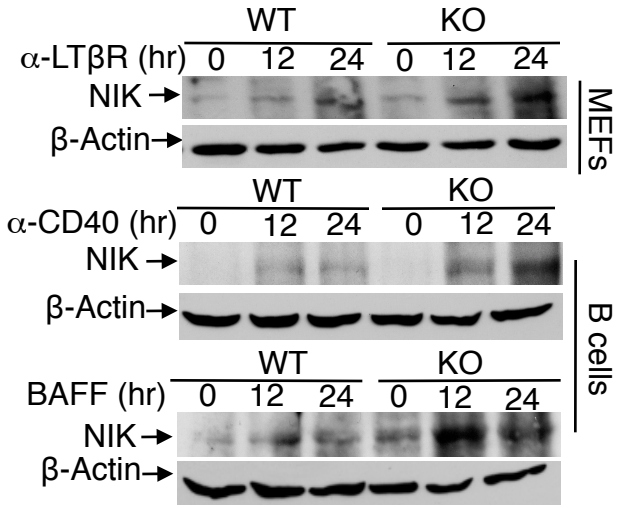

Supplementary Figure 10. NIK induction by noncanonical NF-κB stimuli. IB analysis of NIK and the loading control β-Actin in whole-cell lysates of splenic B cells or primary MEFs, stimulated as indicated. Data are representative of three independent experiments.

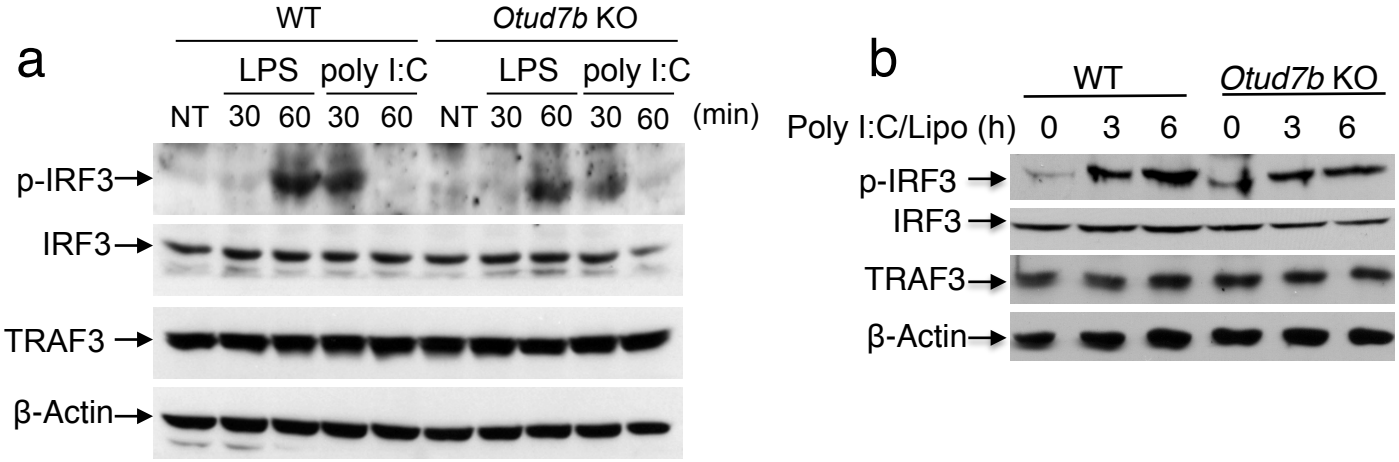

Supplementary Figure 11. The *Otud7b* deficiency does not promote TLR- and RIG-I-stimulated IRF3 activation. a, IB analysis of phosphorylated (p-) and total IRF3, TRAF3, and the loading control β-Actin in whole-cell lysates of WT or *Otud7b*-KO BMDMs stimulated with ligands of TLR4 (LPS) or TLR3 (poly I:C). **b**, IB analysis of WT or *Otud7b*-KO MEFs stimulated via RIG-I using lipofectamine-transfected poly I:C. Data are representative of two independent experiments.

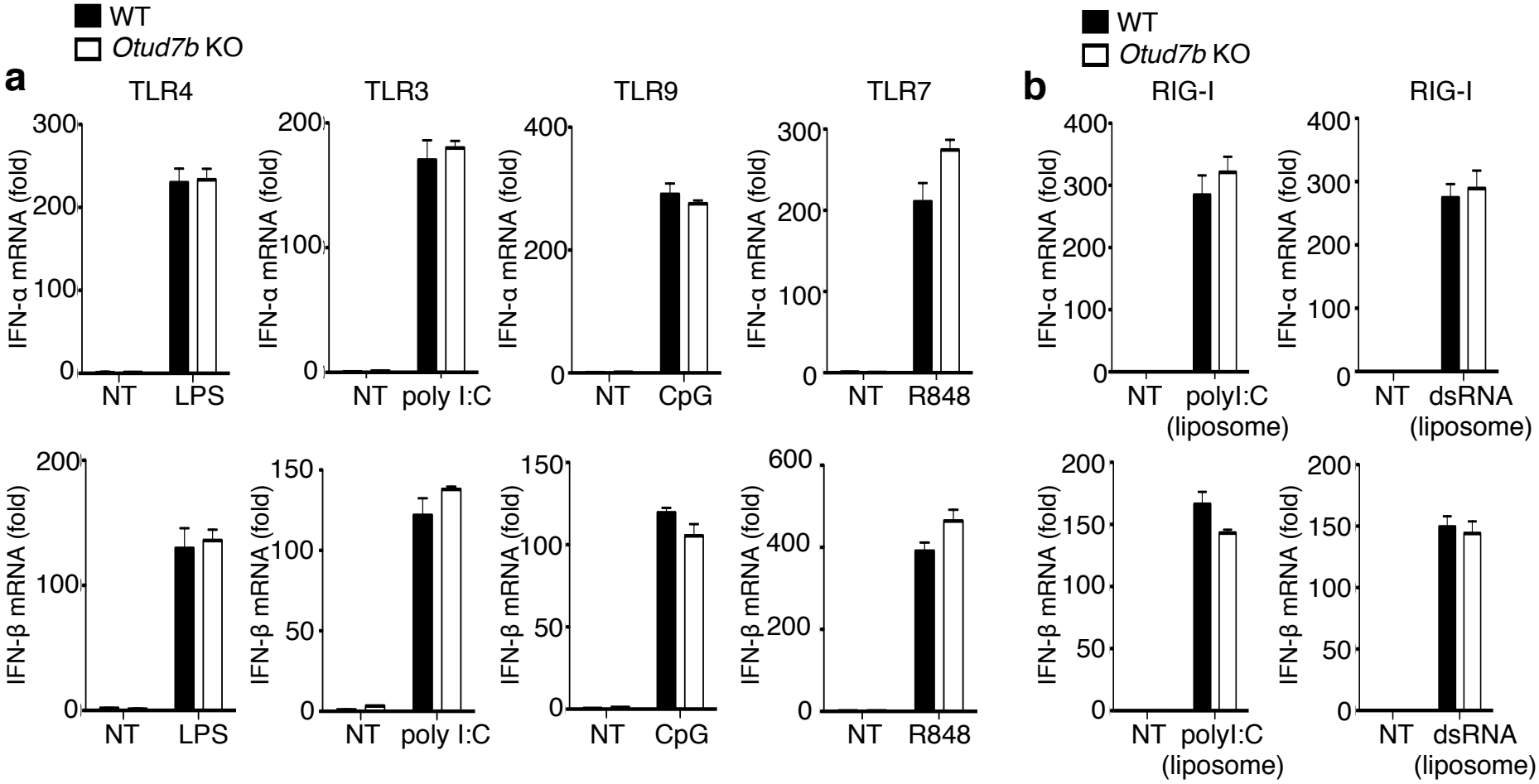

Supplementary Figure 12. *Otud7b* deficiency has no significant effect on type I interferon induction. Wildtype (WT) and *Otud7b*-KO BMDMs (**a**) or MEFs (**b**) were either not treated (NT) or stimulated with the indicated ligands for TLRs or RIG-I. The RIG-I ligands were transfected into the MEFs using a liposome agent, Lipofectamine. The IFNα and IFNβ mRNA level was determined by QPCR and presented as fold of induction relative to the NT cells. Data are representative of three independent experiments.

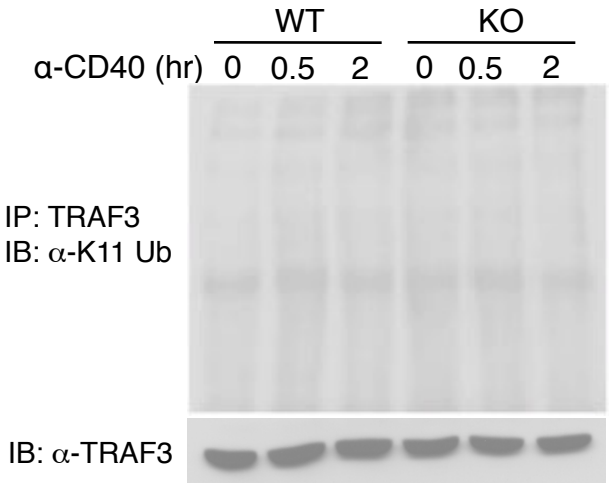

Supplementary Figure 13. K11 ubiquitination of TRAF3. WT or *Otud7b*-KO B cells were stimulated with anti-CD40, in the presence of MG132, for the indicated time periods. TRAF3 was isolated by IP, and its K11 ubiquitination was detected by IB using a K11-specific ubiquitin antibody. The level of TRAF3 protein was detected by IB using anti-TRAF3.

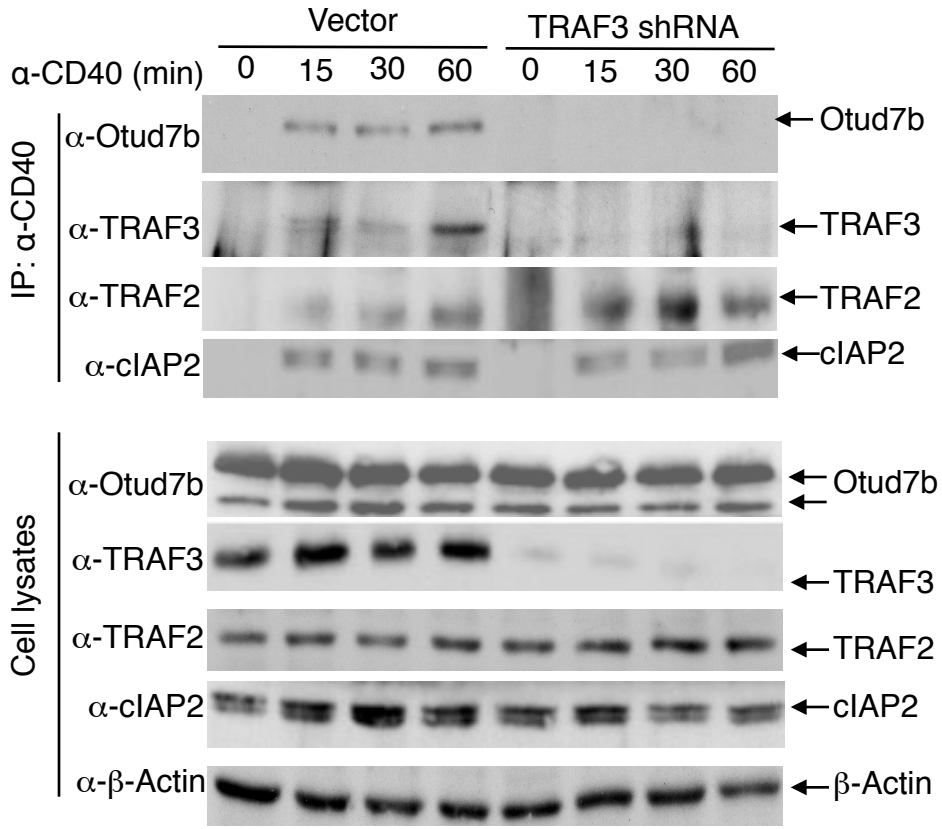

Supplementary Figure 14. TRAF3 is required for Otud7b recruitment to CD40. M12 B cells were infected with either control pGIPZ lentiviral vector or pGIPZ-encoding TRAF3 shRNA. The cells were stimulated with anti-CD40, and the CD40 signaling complex was isolated by IP using anti-CD40, followed by detecting the associated proteins by IB. Protein lysates were also subjected to direct IB to monitor protein expression levels. Data are representative of two independent experiments.

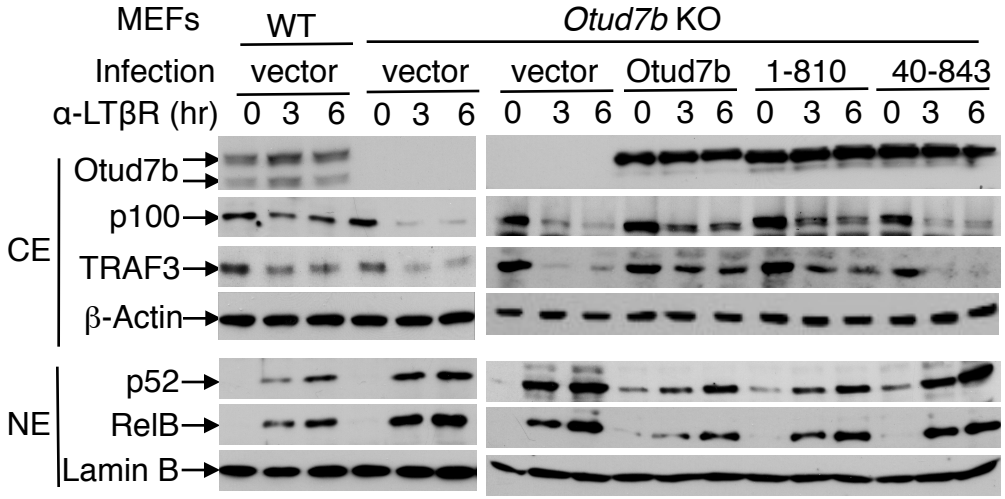

Supplementary Figure 15. The UBA domain of Otud7b is essential for its function. WT or *Otud7b*-KO MEFs were stably infected with pCLXSN(GFP) (vector) or the same vector encoding Otud7b, an Otud7b mutant lacking its C-terminal ZF domain (1-810), or an Otud7b mutant lacking its N-terminal UBA domain (40-843). Following anti-LTβR stimulation, the cells were subjected to IB assays using cytoplasmic (CE) and nuclear (NE) extracts. Note that endogenous, but not exogenous, Otud7b proteins were expressed as two bands. The second band may be generated through alternative translational initiation or alternative splicing. Data are representative of two independent experiments.

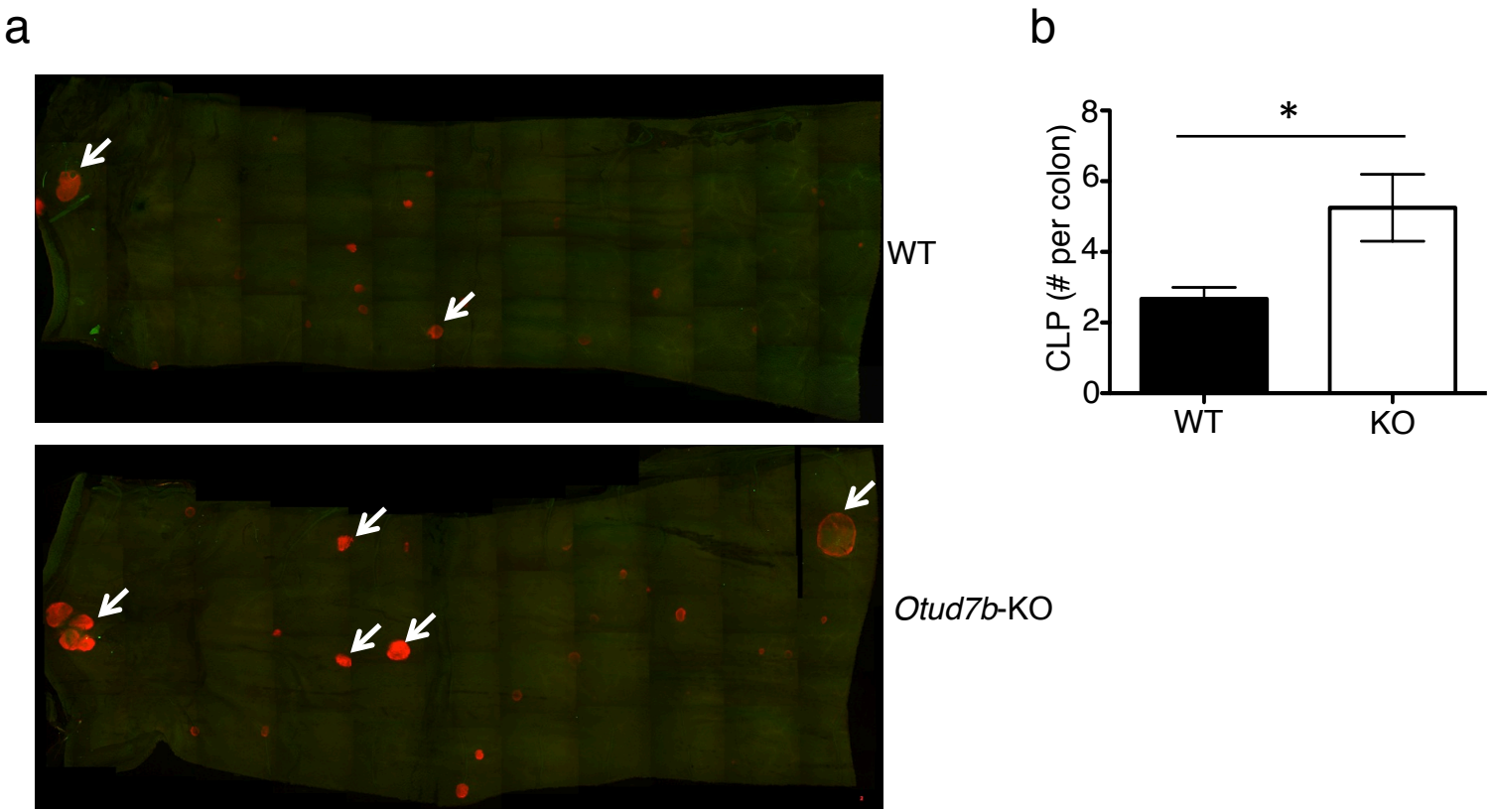

Supplementary Figure 16. Whole-colon imaging to visualize CLPs. Colons were collected, flushed and opened longitudinally along mesenteric border, and fixed in paraformaldehyde. The colons were then stained with Alexa Fluor-647-conjugated anti-B220 and examined by confocal microscopy. SlideBook Software were used to measure the size of B220+ lymphoid follicles, and the follicles bigger than 10,000 μm^2 were considered as CLPs. **a**, A representative picture with the CLPs indicated by arrows. **b**, Summary graph of mean±SD values of CLP numbers. Data represent 4 pairs of age- and gender-match WT and *Otud7b*-KO mice.

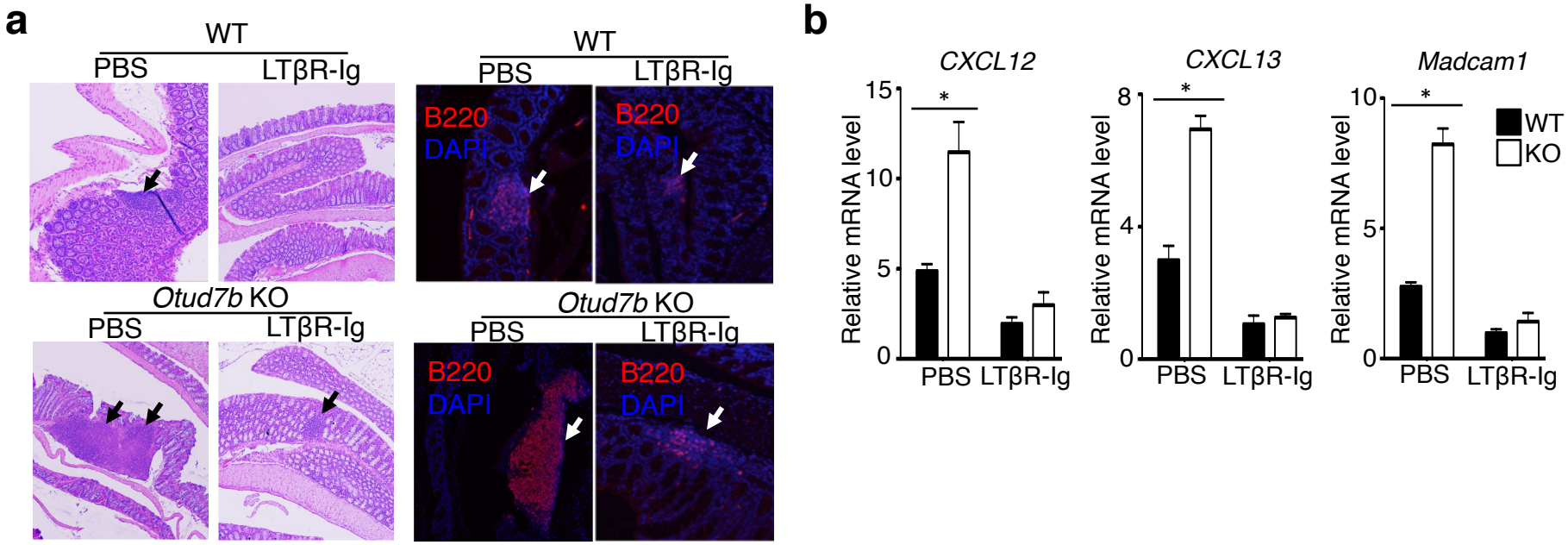

Supplementary Figure 17. Aberrant formation of CLPs in *Otud7b*-KO mice is dependent on LTβR. WT or KO mice were treated i.p. with either PBS or an LTβR fusion protein, LTβR-Ig (100 μg/mouse), on day 0 and day 5 and sacrificed on day 10. **a**, H&E histology analysis (left panel) and immunofluorescence staining using anti-B220 and DAPI nuclear counterstaining (right panel) of colon tissues of WT and *Otud7b*-KO mice. **b**, Real-time QPCR analysis of the indicated genes. Data are representative of three independent experiments, each with four mice per genotype group.

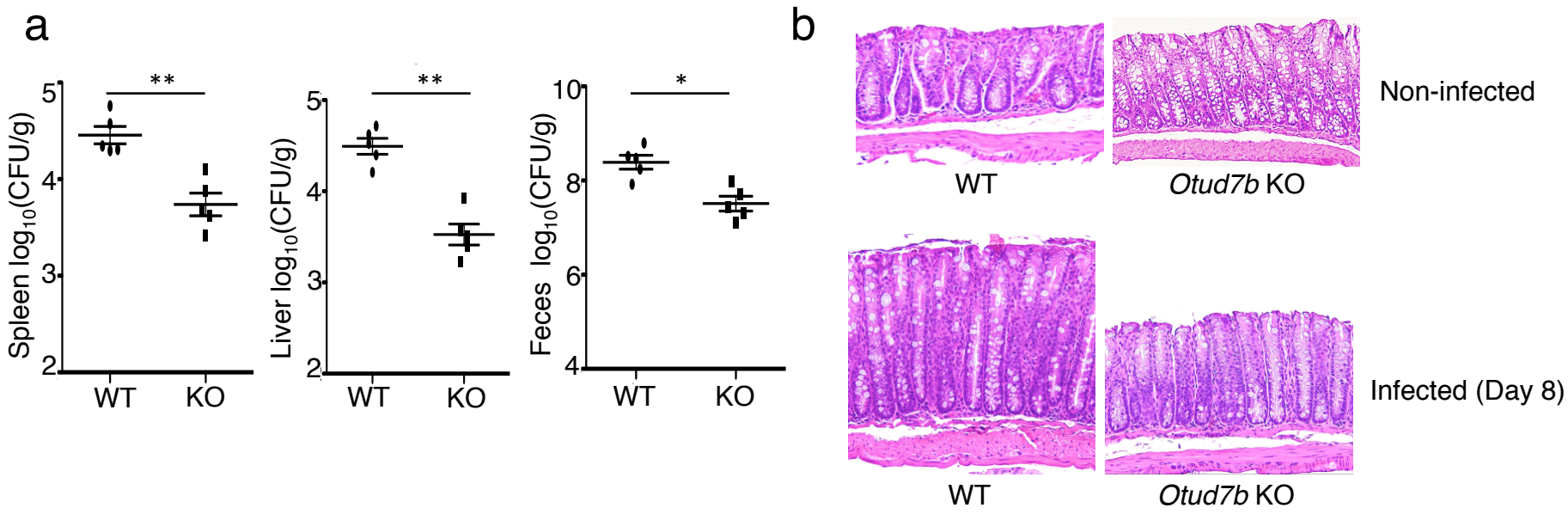

Supplementary Figure 18. *Otud7b* KO mice display elevated mucosal defense against *C. rodentium* infections. WT and *Otud7b*-KO mice were orally infected with *C. rodentium* (4.5 x 10^9). 8 days later, the infected mice, as well as non-infected control mice, were sacrificed for analyzing bacterial burdens in the indicated organs (**a**) and colon histological staining with H&E (**b**). *C. rodentium*-infected colon showed crypt hyperplasia and increased crypt lengths. Data are representative of two independent experiments, each with 3-5 mice per genotype group.

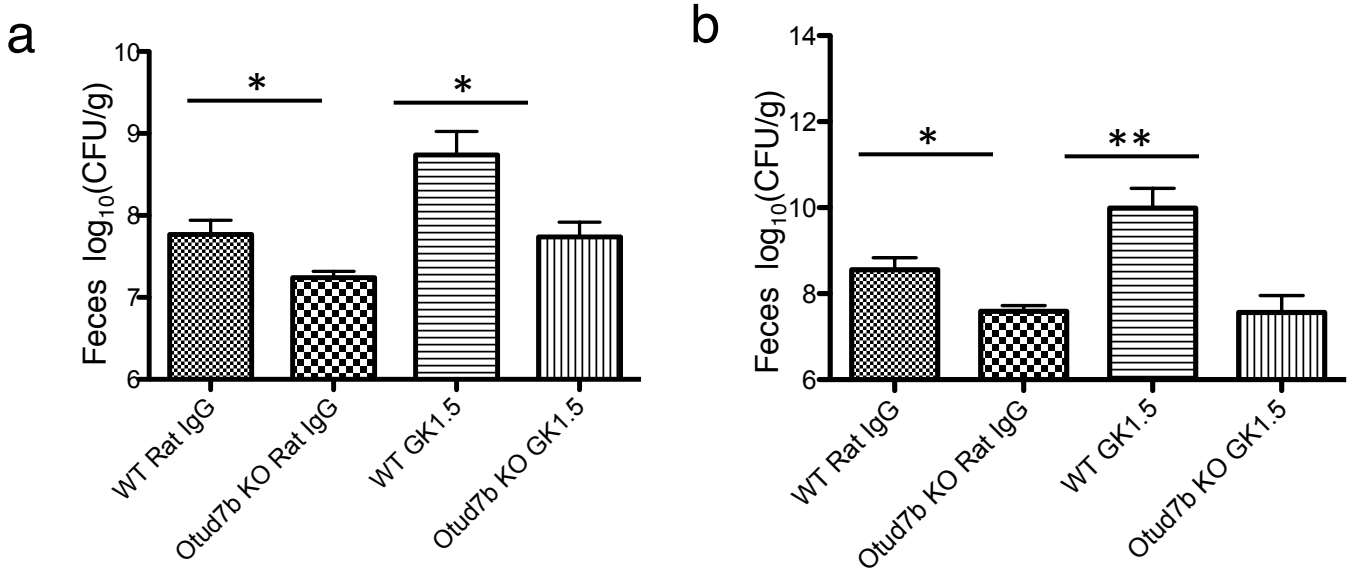

Supplementary Figure 19. Otud7b KO mice are more resistant to *C.rodentium* infection. WT or Otud7b KO mice were infected with 2 x 10^9 *C. rodentium* and injected i.p. with either a control Rat IgG or a rat anti-mouse CD4 antibody (GK1.5) on day 0, 5, and 10. Bacterial burdens were detected in the feces of *C. rodentium*-infected WT and *Otud7b*-KO mice on day 5 (**a**) and day 8 (**b**) after infection. Data are mean±S.D. of 4 mice per group.

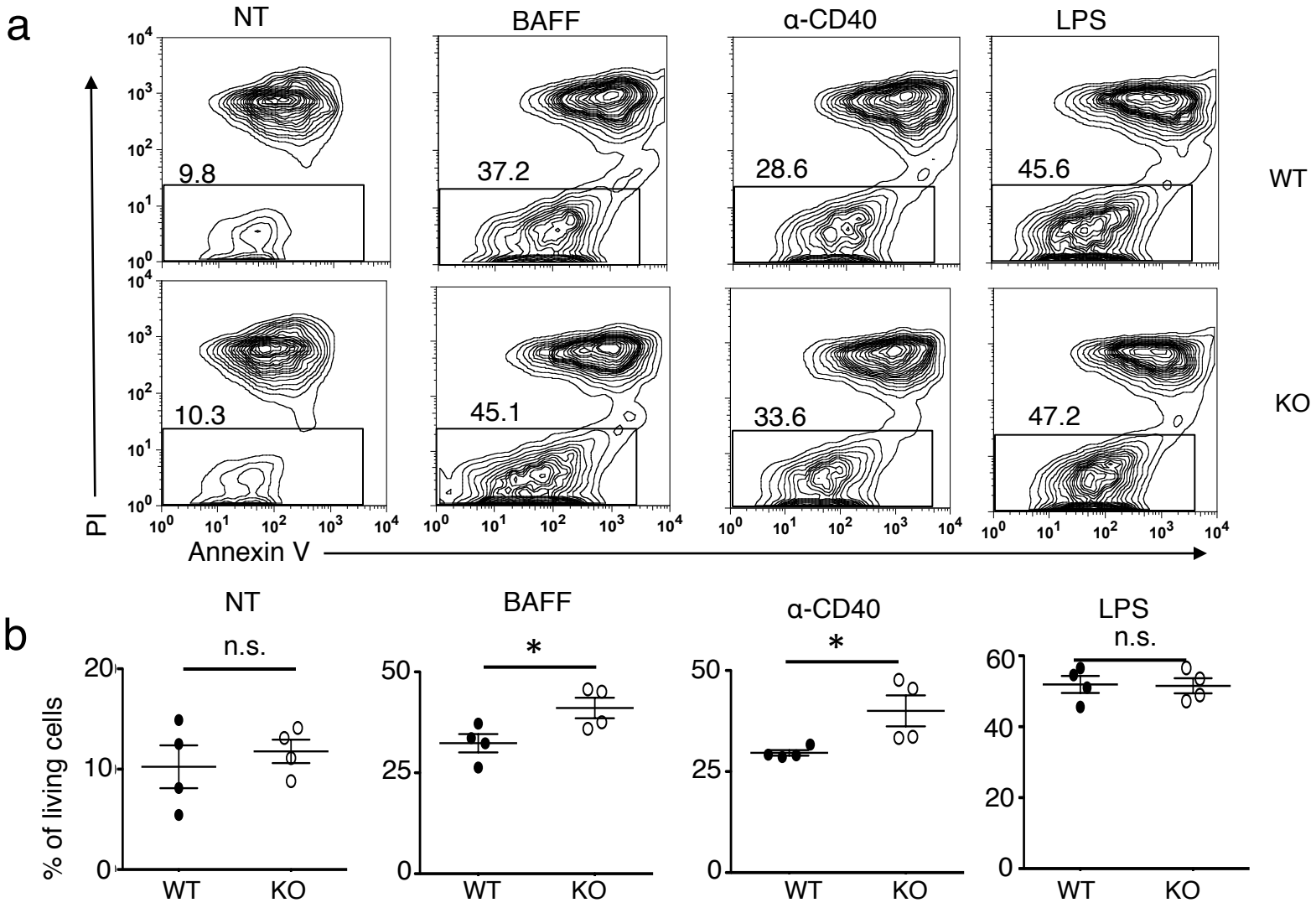

Supplementary Figure 20. Apoptosis of WT and *Otud7b* KO B cells stimulated by different stimuli.
Purified WT and *Otud7b*-KO splenic B cells were cultured for 48 hrs, either in the absence (NT) or presence of the indicated inducers, and subjected to flow cytometry based on staining of Annexin V and propidium iodide (PI) to quantify live cells (double negative cells). Data are presented as a representative flow cytometry plot (**a**) and mean ±S.D. values of multiple mice (with each circle standing for an individual mouse) (**b**). Data are representative for three independent experiments.

Supplementary Table 1. The gene-specific primers used for real-time RT-PCR

Gene	Forward primer	Reverse primer
b-actin	CGTGAAAAGATGACCCAGATCA	CACAGCCTGGATGGCTACGT
MadCam1	GAGCAAGAAGAGGAGATACAAGAG	TGGTGACCTGGCAGTGAAG
Cxcl12	AAGGTCGTCGCCGTGCTG	GATGCTTGACGTTGGCTCTGG
Cxcl13	CAGAATGAGGCTCAGCACAGC	CAGAATACCGTGGCCTGGAG
Ifna	TGCAATGACCTCCATCAGCA	TTCCTGGGTCAGAGGAGGTTC
Ifnb	AGCTCCAAGAAGGACGAACAT	GCCCTGTAGGTGAGGTTGATCT
Aire	CCAGTGAGCCCCAGGTTAAC	GACAGCCGTCACAACAGATGA
Ins1	CTTCAGACCTTGGCGTTGGA	ATGCTGGTGCAGCACTGATC
Cnsa	TTTGCTATGCCCAGACTTCA	TTTCCTCACTGCTGCTATGC
Sp1	GTGTTGCTTGGTGTTTCCAC	GCAGAATCAGCAGTTCCAGA